J Mater Sci: Mater Med (2006) 17:1043–1048
DOI 10.1007/s10856-006-0442-x

Skeletal tissues as nanomaterials

L. Bozec · M. A. Horton

Received: 5 October 2005 / Accepted: 2 February 2006

Abstract Collagen is the most abundant protein in the body and, though the fibre-forming collagens have a 'common' structure, it is adapted to perform a large range of functions—from the differing mechanical needs of tendon versus bone to forming a transparent support structure in the cornea. This perfidy also suggests that collagen could form a generic basis for a range of scaffold needs for tissue engineering or medical device coating applications. We at the London Centre for Nanotechnology—a joint venture between University College London and Imperial College—are taking a bottom-up approach having decided that many of the 'accepted dogmas' of collagen biology may not be quite as soundly based as currently held. We are using several of the tools of 'hard' nanotechnology—such as atomic force microscopy—to re-examine collagen structure with the longer term aim of using such information to design materials with appropriate physical attributes. Examples of our current research on mineralised and soft tissue collagens are presented.

1 Introduction

Skeletal tissues, such as bone, are continually modified by cellular processes in growth, in response to systemic hormones such as oestrogen, and following changes in the mechanical stress to which the skeleton is exposed during everyday life. Bone can be considered as a self-modifying, nano-structured composite material comprising at least two components. The protein part, mainly type I collagen, forms a model for the subsequent deposition of calcium phosphate mineral, hydroxyapatite. The material is 'living' and can be considered to be 'smart' as it self-adapts its structure by way of the function of two types of cells: osteoclasts and osteoblasts. Thus, mineralised bone is removed by osteoclasts during skeletal growth, and in repair after, for example, bone fracture. Calcium is dissolved by cell-mediated acidification of the extra-cellular space, and collagen is degraded following release from osteoclasts of proteolytic enzymes such as cathepsin K. Protein-containing extracellular matrix is then laid down by osteoblasts and this subsequently mineralises. Similar processes occur upon eruption of primary and permanent teeth, during the course of orthodontic tooth movement, or in diseases where the substance of the tooth is damaged. Likewise, tendon is a collagenous tissue that adapts its structure to functional requirements during growth and exposure to differing mechanical strains during exercise; during evolution, adaptive pressures have led to the generation of specialised tendon structure much as occurred for the skeleton [1].

There have been a number of reports on atomic force microscopy (AFM) imaging of mineralised tissues. Mineral and collagen have been studied in bone following artificial removal of calcium using mild acidification or chelation with EDTA [2–4]. We have only found one report [5] where the consequences of osteoclastic resorption upon a mineralised substrate *in vitro* have been examined—however, therein, AFM was only used as a metrology tool to measure the depth of resorption lacunae. We have reported on the purposeful use of osteoclast cell cultures to remove mineral and hence expose collagen for subsequent analysis [6]. Tooth structure has also been examined, generally evaluating the effect of acidification on enamel structure in the context of dental disease [7, 8]. There is also a substantial body of literature examining the detailed structure of the collageneous extracellular

L. Bozec · M. A. Horton (✉)
The Department of Medicine, University College London, London WC1E 6JJ, UK and the London Centre for Nanotechnology, University College London, London WC1E 6BT, UK
e-mail: m.horton@ucl.ac.uk

matrices in tendon [9–11] and non-skeletal tissues, such as in the sclera and cornea [12–14]. In contrast, there is only relatively little work on imaging and mechanical analysis by AFM of collagen at the single molecule level [reviewed in 15–17].

There is renewed interest in understanding the structure-function relationship of one of nature's 'smart' materials in health and disease, the genetic control of its properties, and the identification of any changes that might occur as a consequence of medical treatments. In this paper we review our work on the use of AFM as an analytical tool and demonstrate its value in the structural analysis of tendon, bone and dentine and of its collageneous components. Understanding the structure of native, fully mineralised, skeletal substrates will allow us to investigate the material and morphological properties of bone *in situ* in an unmodified state in health, and in diseases such as osteoporosis where skeletal tissue is mechanically weakened.

2 Material and methods

2.1 Sample preparation

Devitalised 100 μm thick slices of dentine and cortical bone were cut with a diamond saw. Acid treatment was carried out by covering the surface with 7% phosphoric acid for 10 sec, rinsing with deionised water and imaging immediately. Bone samples were cultured with human osteoclasts and dentine with freshly isolated rabbit osteoclasts to expose features in bone by cell-mediated acidification and proteolysis [6]. Resorbing human osteoclasts were generated from blood monocytes on cortical bone for 21 days with differentiation factors M-CSF and RANKL, using conditions that were previously optimised [18]. Any cells remaining after culture were removed by treatment with detergent, washed in distilled water, air dried prior to analysis.

A suspension of native bovine digital tendon collagen fibrils was a gift of Ethicon Inc. (Somerville, NJ, USA) and was dialyzed at 1 mg/ml against 10 mM acetic acid before use and stored at 4°C. For AFM, a 20 μl droplet of the stock solution was deposited onto APTES-treated glass slides for 5 sec, followed by gentle drying with dry N_2.

Purified soluble type I collagen solution (1mg/ml in 0.1M acetic acid; type I rat tail collagen, Sigma Aldrich—UK) was used for single molecule experiments. For imaging, a 40 μl drop of a 1/1000 solution was deposited on freshly cleaved mica (Agar Scientific Ltd.—UK) for 10 min, avoiding evaporation. The sample was rinsed sequentially in phosphate buffered saline and ultra high quality water, and dried with a gentle stream of dry N_2. For single molecule force measurements, higher concentrations of type I collagen were used to increase tip-collagen interaction probability.

2.2 Atomic force microscopy

AFM imaging of mineralised tissues [6, 19] and tendon collagen fibrils were performed using a Dimension 3100 Nanoscope IV AFM (Veeco, Santa Barbara, CA), operated in contact mode with NPS type cantilevers (Veeco, Santa Barbara, CA). The deflection set point was optimised to minimise the contact force in order to reduce sample damage by the AFM probe. Resorption lacunae in dentine or cortical bone produced by osteoclasts were imaged using a Nanowizard AFM (JPK, Berlin, Germany) and NPS type cantilevers. Grain analysis (SPIP software—Image Metrology—Denmark) was performed on the images to obtain the mean diameter of the calcium deposits.

Soluble type I collagen samples were imaged [15] using a Multimode Nanoscope IV AFM (VeecoSanta Barbara, CA), equipped with an E scanner and NSC tips—D lever: ∼28 kHz resonant frequency, ∼0.35 N/m nominal spring constant in air (MikroMaschEstonia). The samples were imaged in dry conditions in tapping mode, with the minimum amplitude set point selected to avoid either damaging or altering the sample on the surface.

Comparative force measurements [15] were performed on a Multimode-Nanoscope IV AFM with a Picoforce attachment (Veeco—Santa Barbara, CA) and on a Molecular Force Puller, MFP1 (Asylum Research—Santa Barbara, CA) using Microlever-D tips: at ∼3.5 kHz resonant frequency, ∼0.03 N/m nominal spring constant (Veeco—Santa Barbara, CA). During the force measurement cycles, a typical load of less than 5 nN was applied at a constant loading rate of 1.8 μm/sec. The resulting force-distance curves were analysed by fitting with the worm-like chain elasticity model [20] to determine the contour length of the molecule.

3 Results and discussion

3.1 Topographic features of collagen monomers

Topographic features of dispersed single type I collagen monomers, as presented in Fig. 1A, were analysed and found to have the following characteristics [15]. First, the contour length of the monomer, 287 ± 35 nm, corresponds to the value quoted in literature from collagen monomers with comparable numbers of residues. Second, the height of the monomer is smaller, ∼0.2 nm, than the theoretical radius of the monomeric collagen triple helix (1.5 nm), whereas the measured width is much larger (∼8 nm) than predicted. These indicate significant effects of substrate interactions

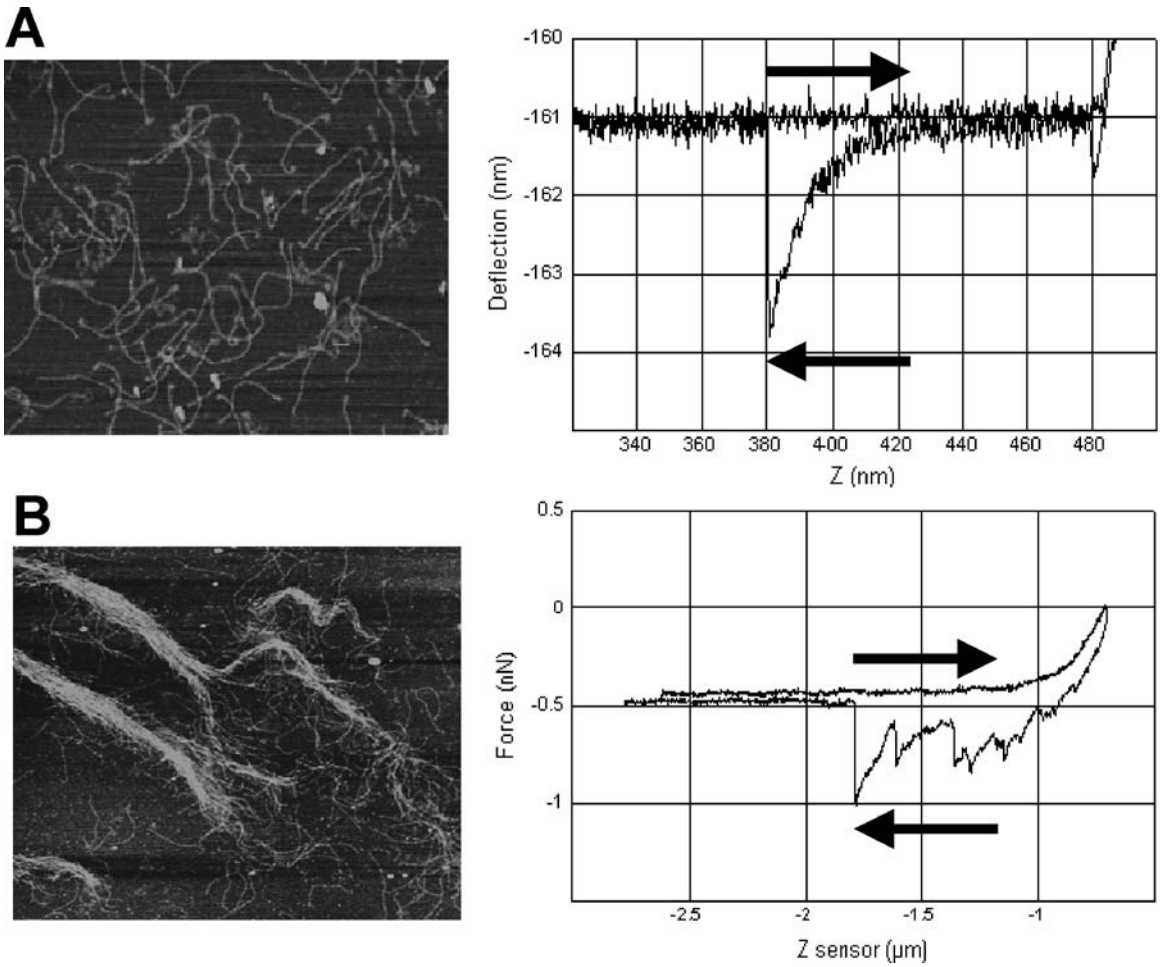

Fig. 1 Topology and mechanical properties of type 1 collagen using atomic force microscopy. (A), Single molecules of type 1 collagen on mica (LH image) (height range = 2 nm); force spectroscopy of collagen showing the force-extension profile of a single molecule of collagen. (B), Aligned type 1 collagen on mica (LH image) (height range = 3 nm); complex 'pulling' pattern due to multiple events

upon collagen structure and/or the effect of compressive mechanical forces from the AFM tip during imaging.

3.2 Pulling on collagen molecules: From simple polymer to complex material

Force versus extension curves were recorded on type I collagen monomers. In most cases, the force curves present a reproducible stretching pattern (Fig. 1A); after the stretching phase, snap-off of the monomer from the probe occurs or of the monomer from the substrate. When the collagen density was greater, spontaneous fibre aggregation and fibrillogenesis occurred (Fig. 1B). Force versus distance curves from such preparations show a more complex profile. They contain features similar to those reported by Gutsmann et al. [16] when studying the stretching pattern of macromolecular complexes of collagen originating from rat tail tendon. The 'simple' force-distance curve set (Fig. 1A) were analysed using a classical entropic treatment such as the worm-like chain model [20]. The mean contour length obtained was found to be 206 nm, smaller than the measured contour length of the monomer (287 nm); this is likely to be due to the picking up of the collagen molecules by the AFM tip being non-covalent and random along its length [15].

3.3 Topology of tendon collagen fibres examined by AFM

We studied the topology of tendon collagen fibres (Fig. 2A) directly by AFM as shown in Fig. 2B and C. Low-resolution images (Fig. 2B) provide an overview at the micron scale of the nature and diversity of the fibres obtained from tendon. It was found that the width of fibres varied between 250 and 410 nm whereas their height ranged from 35 to 60 nm. Nevertheless, all collagen fibres exhibited a common feature: D-banding periodicity (mean ∼69 nm) (Fig. 2C).

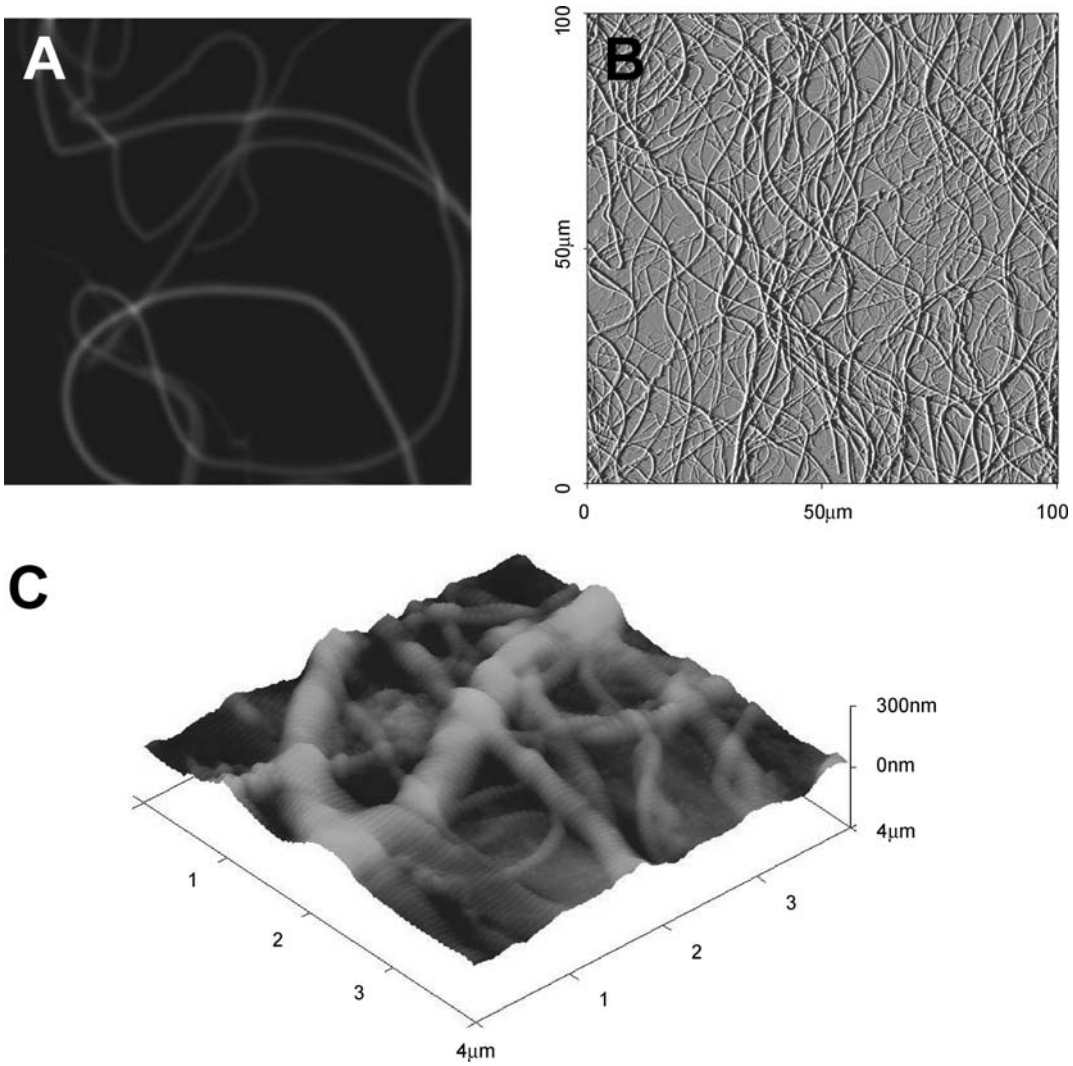

Fig. 2 Topology of tendon collagen. (A), Collagen fibrils from tendon stained with antibody to type I collagen and analysed by fluorescence microscopy. (B), Error atomic force microscope image (100 × 100 μm scan size) of tendon collagen deposited on glass. (C), Pseudo-3D reconstruction of collagen fibrils showing characteristic D-banding (error image, 4 × 4 μm; z range in the simultaneous height image = 300 nm)

3.4 Collagen structure at sites of bone resorption by osteoclasts

Figure 3A shows a low power overview of a resorption lacuna formed by rabbit osteoclasts in dentine, once cells have been removed. Little detail of the exposed mineral or collagen is revealed without further processing. An area of extensive resorption of a bone slice by human osteoclasts is shown in Fig. 3B. No normal bone surface is seen; banded collagen fibrils, aligned in parallel sheets, are easily identified in the deflection image (AFM contact mode). The exposed collagen fibrils in resorption lacunae in bone were analysed in further detail and showed D-periodicity of ∼66 nm size when measured directly, but somewhat lower at ∼64 nm if averaged values across whole images after Fourier analysis (J. de Groot, personal communication). These values correspond with published data [reviewed in 6], obtained from mineralised tissues after acid or EDTA removal of calcium [2–4, 21]. D-periodicity in bone has been reported to range from 61 to 70 nm and is of comparable size to that obtained from collagen fibrils from tendon and other non-skeletal tissues [12–14].

We also analysed fibril diameter in the same specimens; these ranged from 52 to 74 nm in bone. It is interesting to note that measured values of fibre diameter obtained using other methods vary in the published literature from 30 to 120 nm [22, 23]. The effect of hydration on fibril diameter has been discussed previously. Habelitz et al. [24] measured hydrated and dehydrated fibrils in dentine. While the hydrated collagen fibrils had diameters varying in the range 75 to 105 nm, the dehydrated fibrils showed a narrower distribution of diameters; this is due to a partial swelling of the fibre as it is

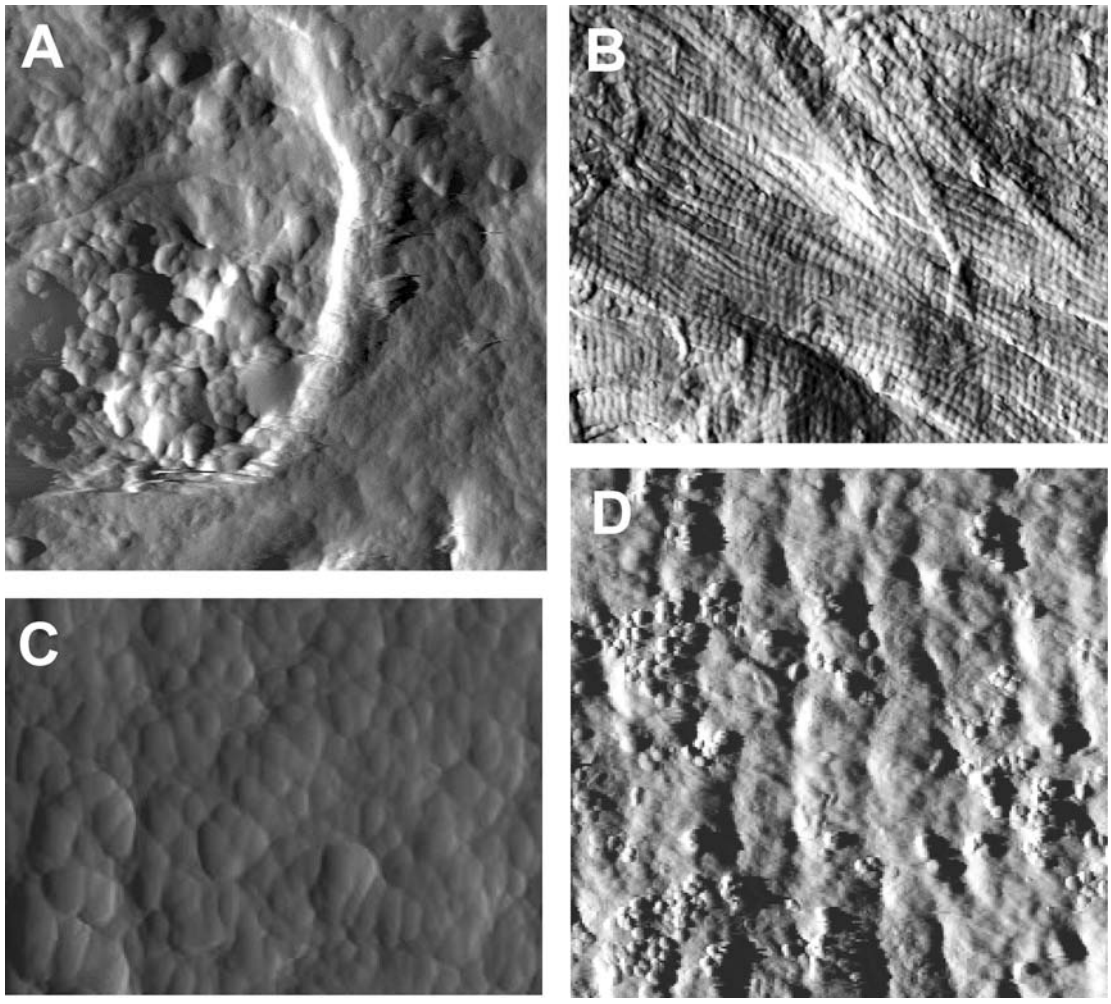

Fig. 3 Atomic force microscopy of mineralised tissues. (A), Error image ($20 \times 20\ \mu$m; z range in the simultaneous height image = 11 μm) of a resorption lacuna formed by osteoclasts cultured on dentine. (B), $2 \times 2\ \mu$m error image of an area of resorbed cortical bone showing pleats of parallel collagen fibres with characteristic D-banding (periodicity ~69 nm). (C), Areas of hydroxyapatite crystals on the cut surface of cortical bone (error image, $3 \times 3\ \mu$m scan). D, Acid etched dentine showing tangentially cut dentine tubules and mineral spherules (error image, $40 \times 40\ \mu$m scan)

being hydrated. There is also a concomitant alteration in D-banding: an axial D-periodicity of approximately 65 nm has been reported in collagen fibrils when examined dehydrated, compared to the value of 67 nm when hydrated. Further, El Feninat [2] reported the disappearance of collagen fibres from etched dentine when vacuum dried. This means that dehydration results in both shrinkage and structural change in the fibrils.

3.5 Atomic force microscopy of native bone and dentine surfaces

AFM imaging of unmodified cortical bone shows detail of mineral structure [19], observed as approximately round crystals with a mean diameter of about 225 nm (Fig. 3C). AFM was also performed on dentine immediately after treatment with phosphoric acid (Fig. 3D). Dentine tubules—longitudinally and tangentially cut [19]—are clearly visible; again collagen fibres are not seen without further treatment such as by osteoclastic resorption (*vide supra*) or following acid treatment. Clusters of mineralised spherical structures were seen against a smoother background, suggesting an inhomogeneous mineralisation with the spherules being more resistant to dissolution, and ranged in size from 0.8 to 1.4 μm [19].

4 Conclusions

We performed single molecule force spectroscopy of soluble type 1 collagen molecules on mica and revealed a diversity of features—from worm-like chain single molecule extension to complex profiles indicative of multiple interacting events [15]. Tendon collagen fibril topology was examined; these varied around 300 nm in width and showed D-banding

periodicity of about 69 nm. AFM was also used to examine the topology of collagen and mineral in samples of cortical bone and ivory dentine [6, 19]. The general morphological features of the two tissues, usually observed in phase or stained histological preparations, were easily identifiable in AFM scans. Moreover, mineral crystals were observed in high magnification scans, and collagen with an axial D-periodicity was observed in bone within resorption lacunae formed *in vitro* in bone by osteoclasts; values for collagen periodicity fit those in the published literature.

Our results suggest that AFM is a useful tool for the study of collagenous tissues and may be an asset to our understanding disease processes. It is known that the gross structural and mechanical properties of bone are altered in osteoporosis; however, there is only limited information on the collagen and mineral structural changes at the nanoscale that accompany bone pathology. Likewise, collagen structure in tendon deserves further study, especially in the context of understanding its mechanical properties in the face of increased use of collagen-based materials in tissue engineering and biomedical device coatings.

Acknowledgment An award of a programme grant to M.A.H. from the Wellcome Trust, UK funded this work. We thank Brian Nicholls for performing the bone resorption experiments.

References

1. D. A. W. THOMPSON, "On Growth and Form," edited by J. T. Bonber (Cambridge University Press, 1961).
2. F. EL FENINAT, T. H. ELLIS, E. SACHER and I. STANGEL, *J. Biomed. Mater. Res.* **42** (1998) 549.
3. G. W. MARSHALL, Y. J. CHANG, S. A. GANSKY and S. J. MARSHALL, *J. Dent. Res*. **77** (1998) 32.
4. G. W. MARSHALL, I. C. WU-MAGIDI, L. G. WATANABE, N. INAI, M. BALOOCH, J. H. KINNEY and S. J. MARSHALL, *J. Biomed. Mater. Res*. **42** (1998) 500.
5. K. DEBARI, T. SASAKI, N. UDAGAWA and B. R. RIFKIN, *Calcif. Tissue Int*. **56** (1995) 566.
6. L. BOZEC, J. DE GROOT, M. ODLYHA, B. NICHOLLS, S. NESBITT, A FLANAGAN and M. HORTON, *Ultramicrosc*. (2005) in press.
7. O. SOLLBOHMER, K. P. MAY and M. ANDERS, *Thin Solid Films* **264** (1995) 176.
8. F. H. JONES, *Surf. Sci. Reps.* **42** (2001) 79.
9. D. BASELT, J. REVEL and J. BALDESCHWIELER, *Biophys. J*. **65** (1993) 2644.
10. I. REVENKO, F. SOMMER, D. T. MINH, R. GARRON and J. M. FRANC, *Bio. Cell*. **80** (1994) 67.
11. T. GUTSMANN, G. E. FANTNER, M. VENTURONI, A. EKANI-NKODO, J. B. THOMPSON, J. H. KINDT, D. E. MORSE, D. K. FYGENSON and P. K. HANSMA, *Biophys. J.* **84** (2003) 2593.
12. K. M. MEEK and N. J. FULLWOOD, *Micron* **32** (2001) 261.
13. D. MELLER, K. PETERS and K. MELLER, *Cell Tissue Res*. **288** (1997) 111.
14. S. YAMAMOTO, J. HITOMI, S. SAWAGUCHI, H. ABE, M. SHIGENO and T. USHIKI, *Jpn. J. Ophthalmol*. **46** (2002) 496.
15. L. BOZEC and M. HORTON, *Biophys J*. **88** (2005) 4223.
16. T. GUTSMANN, G. E. FANTNER, J. H. KINDT, M. VENTURONI, S. DANIELSEN and P. K. HANSMA, *Biophys. J*. **86** (2004) 3186.
17. J. B. THOMPSON, J. H. KINDT, B. DRAKE, H. G. HANSMA, D. E. MORSE and P. K. HANSMA, *Nature* **414** (2001) 773.
18. C. S. LADER, J. SCOPES, M. A. HORTON and A. M. FLANAGAN, *Brit. J. Haem.* **112** (2001) 430.
19. L. BOZEC, J. DE GROOT, M. ODLYHA, B. NICHOLLS and M. A. HORTON, *IEE Proceedings: Nanobiotechnology* (2005) in press.
20. C. BUSTAMANTE, J. F. MARKO, E. D. SIGGI and S. SMITH, *Science* **265** (1994) 1599.
21. T. SASAKI, K. DEBARI and M. HASEMI, *J. Electron Microsc*. **42** (1993) 356.
22. J. K. AVERY, "Oral Development and Histology" (B.C. Dekker Inc., Toronto, Philadelphia, 1988).
23. C. P. LIN, W. H. DOUGLAS and D. S. L. ERLANDSEN, *J. Histochem. Cytochem.* **41** (1993) 381.
24. S. HABELITZ, M. BALOOCH, S. J. MARSHALL, G. BALOOCH and G. W. MARSHALL, *J. Struct. Biol*. **138** (2002) 227.